Surporting Information

Two 1D carboxylate–bridged magnets displaying solvent-dependent canted antiferromagnetic ordering

Zhong-Yi Li,* Wen-Jing Wang, Dong-Qing Wu, Chi Zhang, Fu-Li Zhang, Bin Zhai* and Jian-Jun Zhang*

Materials and Physical measurements. All chemicals were obtained from commercial sources and used without further purification. Elemental analyses were determined by a Vario EL III elemental analyzer. FT-IR spectra were recorded in the range of 4000-400 cm^{-1} on a JASCO FT/IR-430 spectrometer with KBr pellets. Powder X-ray diffraction (PXPD) measurements were carried out on a Bruker D8 ADVANCE X-ray Diffractometer using Cu Kα (λ = 1.5418 Å) at room temperature. Thermogravimetric analyses were performed under a flow of nitrogen (40 mL/min) at a ramp rate of 10 °C/min, using a NETZSCH STA 449F3 instrument. Magnetic measurements were performed on a Quantum Design SQUID magnetometer MPMS XL-7. The data was corrected for the sample holder and the diamagnetic contributions.

Table S1. Selected bond lengths (Å) and angles (°) for **1**.

Mn1-O1	2.096(2)	Mn1-O6C	2.190(2)
Mn1-O2A	2.167(2)	Mn1-O9	2.205(2)
Mn1-O5	2.1865(18)	Mn1-O5B	2.2681(18)
O1-Mn1-O2A	88.02(8)	O5-Mn1-O9	165.65(8)
O1-Mn1-O5	97.89(9)	O6C-Mn1-O9	85.56(8)
O2A-Mn1-O5	85.08(8)	O1-Mn1-O5B	165.29(8)
O1-Mn1-O6C	85.91(8)	O2A-Mn1-O5B	104.76(7)
O2A-Mn1-O6C	168.19(8)	O5-Mn1-O5B	76.40(7)
O5-Mn1-O6C	105.78(8)	O6C-Mn1-O5B	82.72(7)
O1-Mn1-O9	91.56(10)	O9-Mn1-O5B	96.82(8)
O2A-Mn1-O9	84.48(8)		

Symmetry codes: A, 1+x, y, z; B, 3-x, 1-y, 2-z; C, 2-x, 1-y, 2-z.

Table S2. Selected bond lengths (Å) and angles (°) for **2**.

Mn1-O1	2.106(2)	Mn1-O6C	2.1999(18)
Mn1-O5	2.1700(17)	Mn1-O9	2.216(2)
Mn1-O2A	2.1808(19)	Mn1-O5B	2.2340(17)
O1-Mn1-O5	99.08(8)	O2A-Mn1-O9	89.40(8)
O1-Mn1-O2A	86.34(8)	O6C-Mn1-O9	82.51(8)
O5-Mn1-O2A	89.38(7)	O1-Mn1-O5B	171.18(8)
O1-Mn1-O6C	86.43(8)	O5-Mn1-O5B	75.77(6)
O5-Mn1-O6C	99.92(7)	O2A-Mn1-O5B	100.62(7)
O2A-Mn1-O6C	169.02(7)	O6C-Mn1-O5B	87.41(7)
O1-Mn1-O9	91.38(10)	O9-Mn1-O5B	94.08(8)
O5-Mn1-O9	169.37(8)		

Symmetry codes: A, 1+x, y, z; B, 2-x, 1-y, 1-z; C, 1-x, 1-y, 1-z.

Table S3. Selected hydrogen bond lengths (Å) and bond angles (°) in **1**.

D-H	d(D-H)	d(H..A)	∠DHA	d(D···A)	A	Symmetry Code
O9-H9C	0.818	2.093	170.43	2.902	O8	[x+1, y-1, z]
O9-H9D	0.85	1.911	163.5	2.736	O7	[-x+3, -y+1, -z+2]
C13-H13	0.93	2.362	138.68	3.122	O3	

Table S4. Selected hydrogen bond lengths (Å) and bond angles (°) in **2**.

D-H	d(D-H)	d(H..A)	∠DHA	d(D···A)	A	Symmetry Code
C6-H6	0.93	2.242	173.93	3.168	O7	
C13-H13	0.93	2.731	145.63	3.537	O9	[-x+2, -y+1, -z+1]

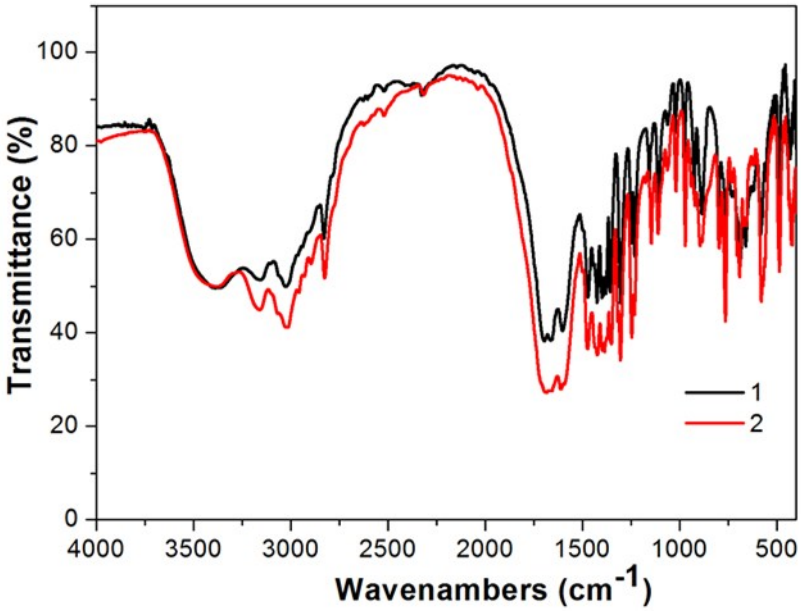

Fig. S1. The IR spectra of **1** and **2**.

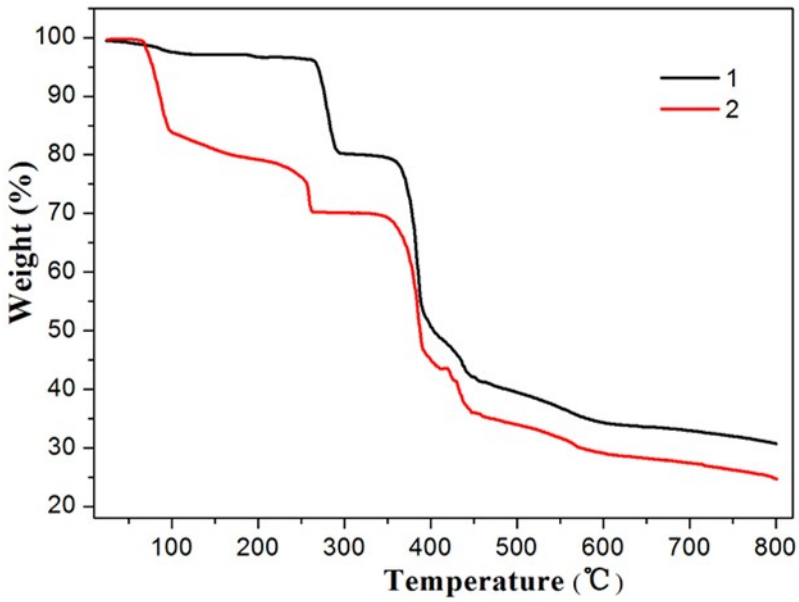

Fig. S2. TG curves for **1** and **2** in a nitrogen atmosphere (10 °C/min).

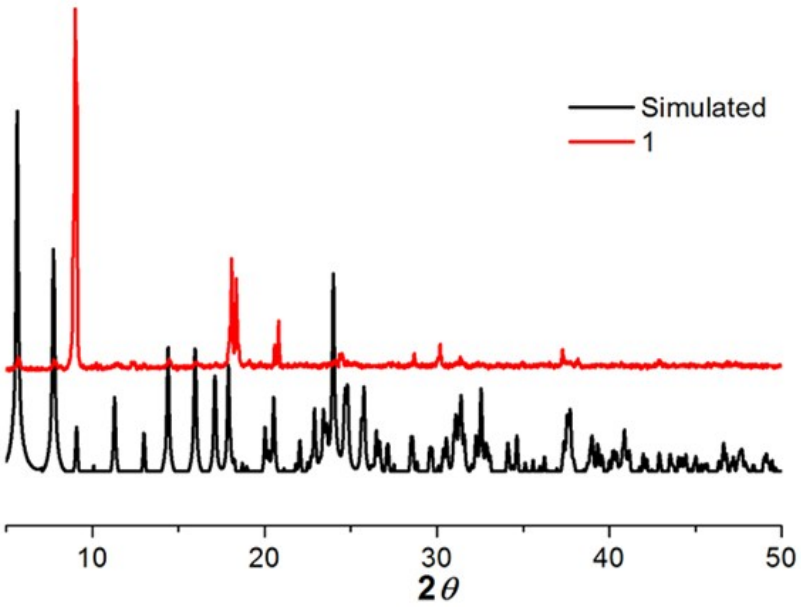

Fig. S3. Powder X-ray diffraction patterns of **1**.

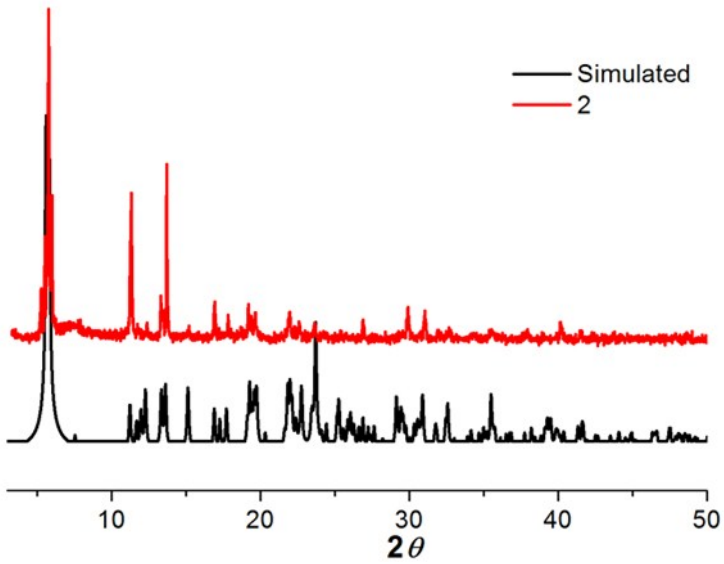

Fig. S4. Powder X-ray diffraction patterns of **2**.

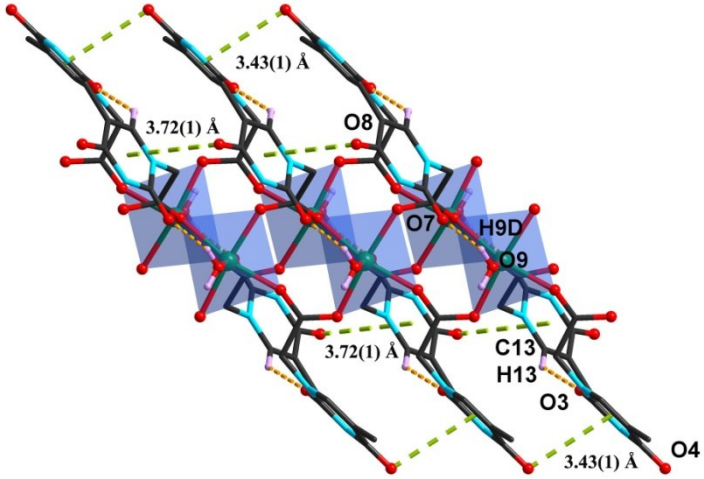

(a)

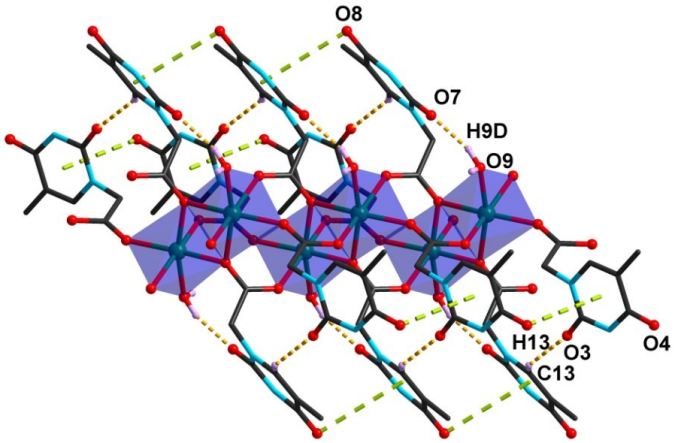

(b)

Fig. S5. The 1D chain structure of **1** viewed along *b* axis (a) and [011] axis (b). H bonding: light orange dotted lines; π−π interaction: lime dotted lines.

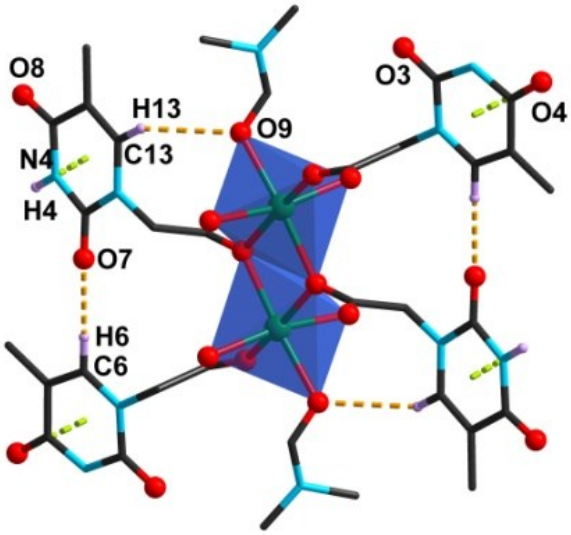

Fig. S6. View of the 1D chain structure of **2** along *a* axis (H bonding: light orange dotted lines; π−π interaction: lime dotted lines).

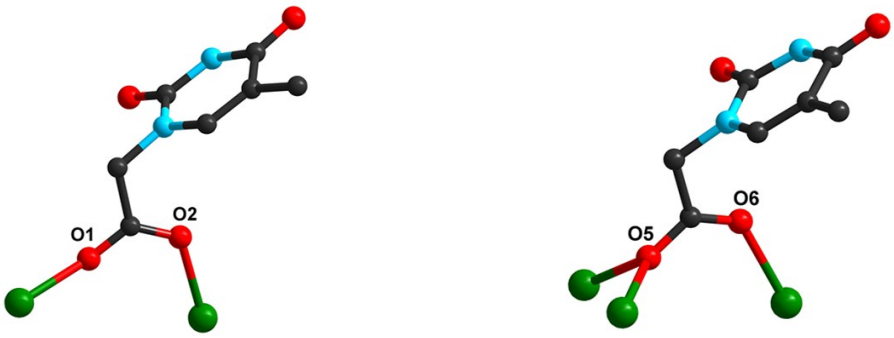

I II

Fig. S7. Coordinate modes of TAc^- ligands in **2**.

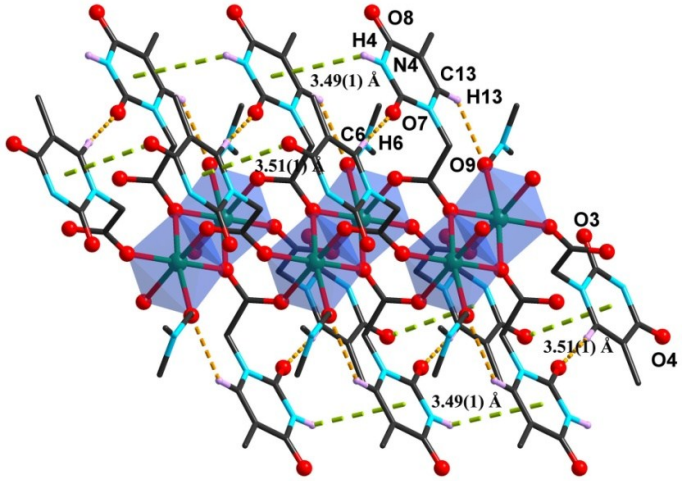

(a)

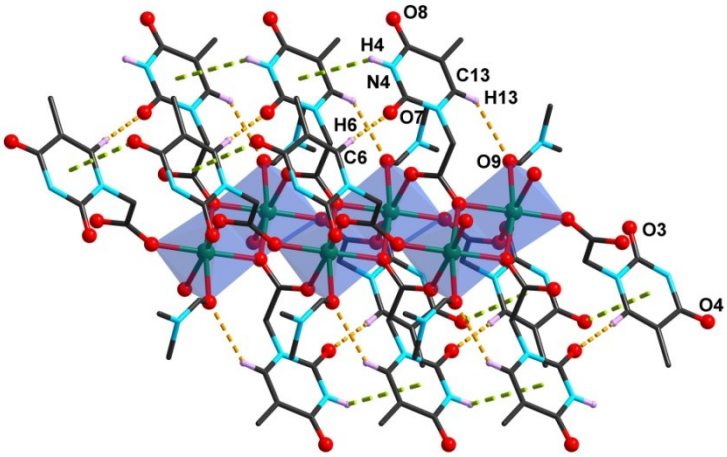

(b)

Fig. S8. The 1D chain structure of **2** viewed along *c* axis (b) and [101] axis (c). H bonding: light orange dotted lines; π−π and N-H−π interactions: lime dotted lines.

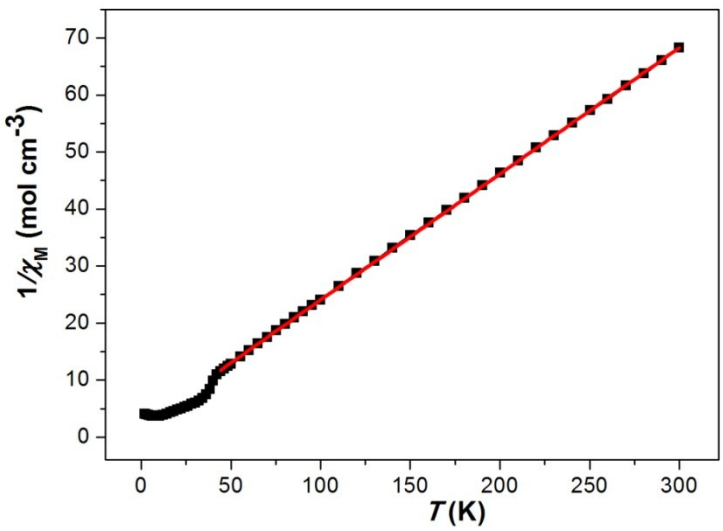

Fig. S9. Temperature dependence of the $1/\chi_M$ values for **1** at 1000 Oe dc magnetic field. The red solid line represents the best fit to the data between 44 and 300 K.

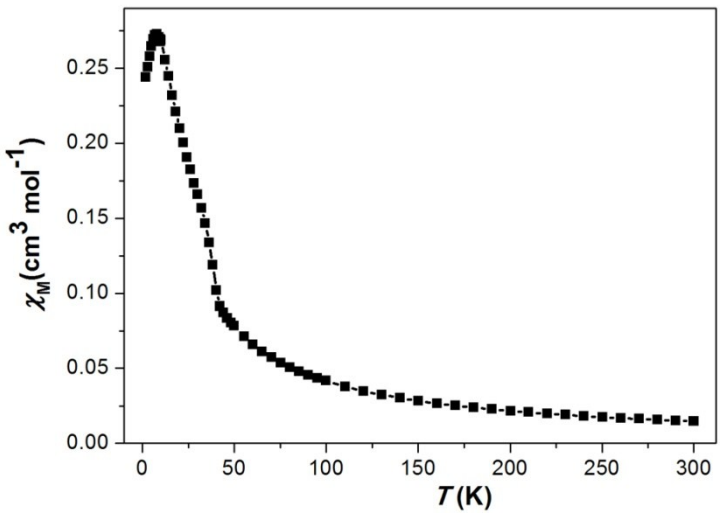

Fig. S10. Temperature dependence of the χ_M values for **1** at 1000 Oe dc magnetic field.

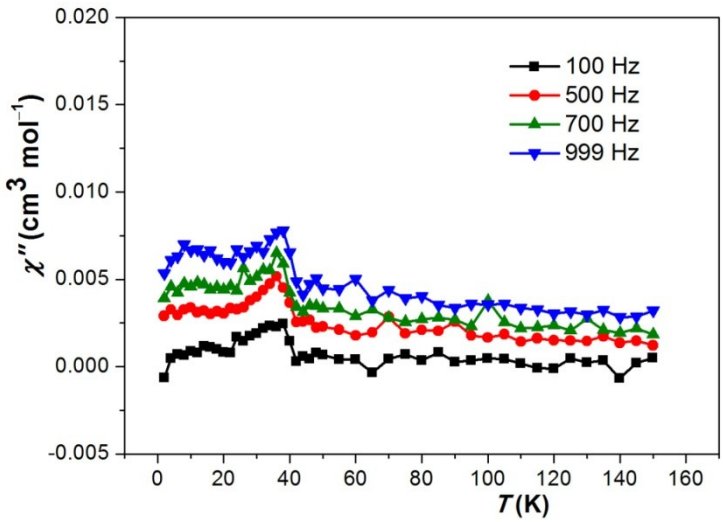

Fig. S11. Temperature dependence of the χ″ ac susceptibility for **1** at the indicated frequencies and in the zero dc field.

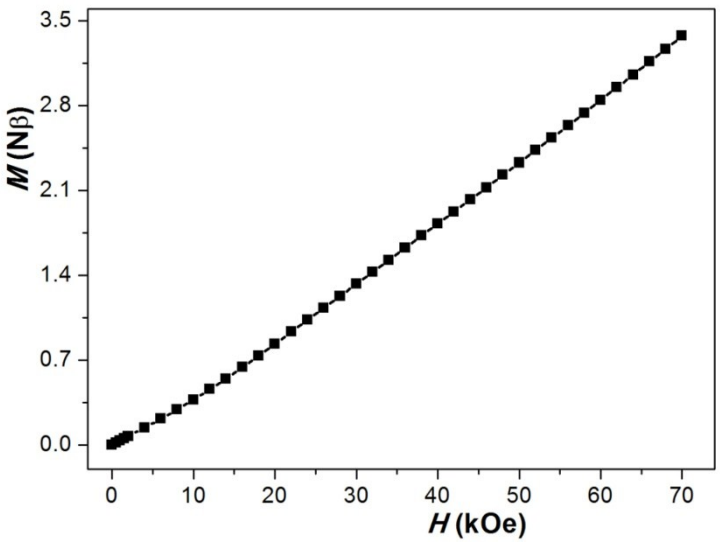

Fig. S12. Field dependence of the magnetization of **1** at 2.0 K.

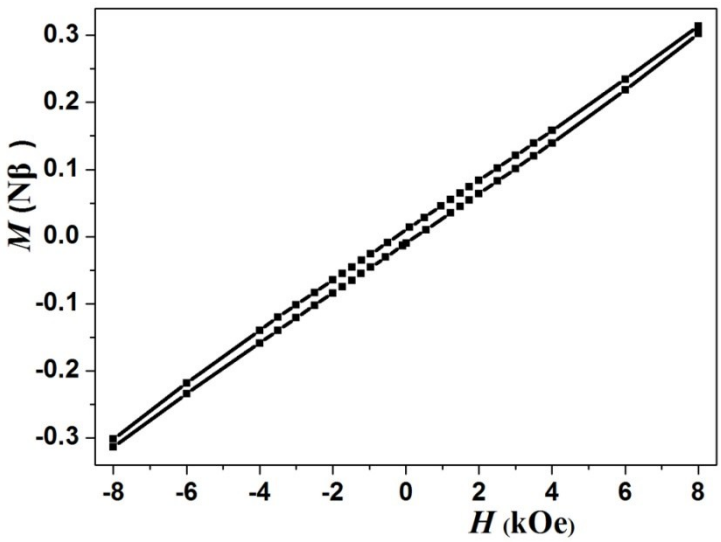

Fig. S13. magnetic hysteresis loop for **1** measured at 2.0 K.

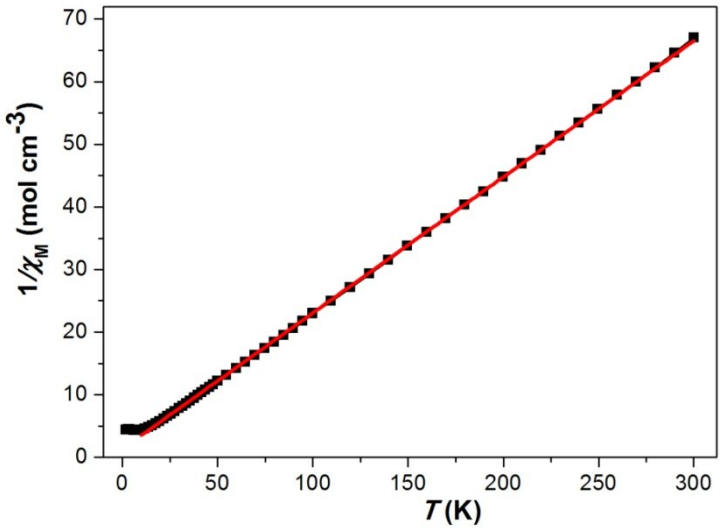

Fig. S14. Temperature dependence of the $1/\chi_M$ values for **2** at 1000 Oe dc magnetic field. The red solid line represents the best fit to the data between 10 and 300 K.

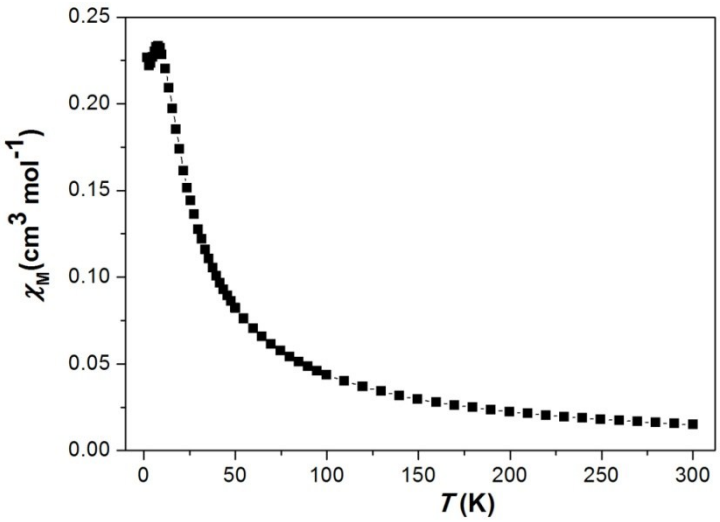

Fig. S15. Temperature dependence of the χ_M values for **2** at 1000 Oe dc magnetic field.

Fig. S16. Field dependence of the magnetization of **2** at 2.0 K.

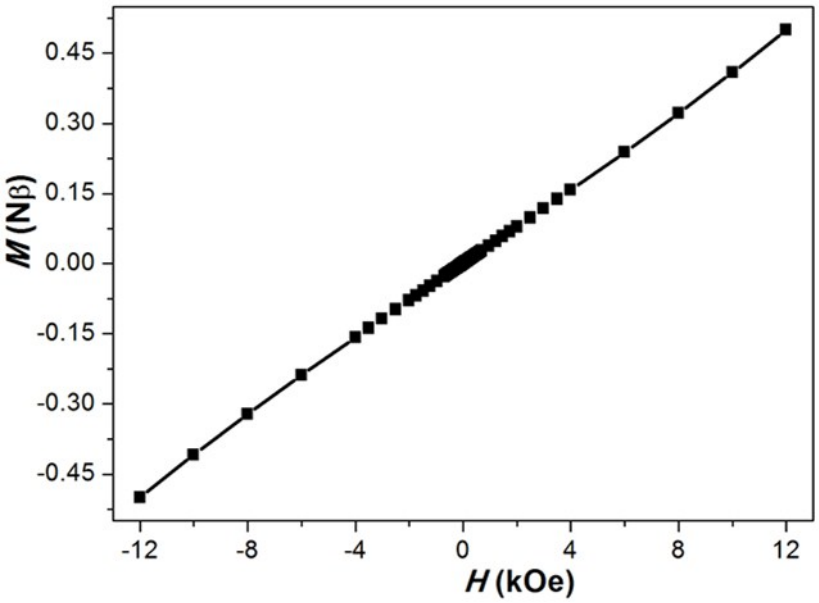

Fig. S17. magnetic hysteresis loop for **2** measured at 2.0 K.